

# SANS of interacting magnetic micro-sized Fe particles in a Stomaflex creme polymer matrix

M. BALASOIU<sup>a</sup>, E. M. ANITAS<sup>b\*</sup>, I. BICA<sup>b</sup>, R. ERHAN<sup>a</sup>, V. A. OSIPOV, O. L. ORELOVICH, D. SAVU<sup>b</sup>, S. SAVU<sup>b</sup>, A. I. KUKLIN

*Joint Institute for Nuclear Research, 141980 Dubna, Moscow region, Russian Federation*

*<sup>a</sup>Horia Hulubei National Institute of Physics and Nuclear Engineering, Bucharest, Romania*

*<sup>b</sup>The West University of Timisoara, Blvd. V. Parvan, No. 4, 300223 Timisoara, Romania*

We report investigations results obtained from small angle neutron scattering on magnetic elastomers polymerised with and without magnetic field at 25%, 50% and 75% mass concentration of Fe particles with a mean radius of 2.09  $\mu\text{m}$  inside a polymer matrix of stomaflex creme. The magnetic field used in polymerisation process is 156.5 mT. The profiles of the curves have a similar behavior for each concentration, showing that for these sizes of particles and polymerisation process at 156.5 mT, the microstructure of magnetic elastomers is the same in the  $q$ -range of 0.006 – 0.1  $\text{\AA}^{-1}$ , and scattering intensities increase proportionally with increasing the mass-concentration of Fe particles.

(Received October 1, 2008; accepted October 6, 2008)

*Keywords:* SANS, Magnetic elastomers, Fractals, Polymers, Polydimethylsiloxane, Fe particles

## 1. Introduction

The main advantage of composite materials resides in the possibility of combining physical properties of the constituents to obtain new structural or functional properties. The scientific efforts in this field were therefore focused to the comprehension and optimization of the structural performances of these materials. Increased demand for high performance control design in combination with recent advances in condensed matter physics have produced a class of systems termed smart, intelligent or adaptive. Magnetic elastomers are a class of smart materials which consist of polymers with nano-micro sized particles, and show a great promise for many industrial and technological applications, due to the enhanced properties compared with classic materials. Therefore informations on the microstructure of such materials are very useful for understanding their behavior in different limiting conditions as required by industry and technology. The reinforcement of polymeric matrix with fine-particle metallic fillers to improve the physical properties (magnetic susceptibility, electrical conductivity etc) of polymeric materials [1] is widely used in industry.

A precise description of the microscopic structure from electron or atomic force microscopy techniques is often difficult to obtain. Scattering techniques [2, 3] (neutrons, X-rays, light) are proved to be a very powerful tool for investigation the microstructure, organization and dynamics of matter. This is because the physical quantities, averaged over the whole sample (i.e. radius of gyration, specific surface), can be extracted with almost no approximation or model. Particularly, small-angle neutron scattering (SANS) [4, 5], is suitable for structural analysis and it is the method used in this paper to reveal the

structure of stomaflex creme polymer filled with Fe particles. The obtained information's from the SANS curves serves a lot of purposes ranging from understanding the way in which particles are distributed in the polymer matrix till the possibility of controlling certain material properties. For magnetic elastomers the SANS is a result of the interactions between neutrons and atomic nuclei (nuclear scattering) from one hand, and interactions between magnetic moments of neutrons and magnetic atoms (magnetic scattering) from another hand.

In this paper the study was conducted to determine the effect of embedding of Fe micro-sized particles, in a Stomaflex creme polymer matrix, polymerized in zero field and polymerized in magnetic field; on the small-angle neutron scattering curve from magnetic elastomers.

## 2. Experimental

Magnetic elastomers systems analyzed here, obtained from reinforcement of spherical Fe particles [6] into a polymer matrix of Stomaflex Crème [Fig. 1 and Fig. 2], were prepared at the Faculty of Physics, The West University of Timisoara by Prof. I. Bica.

Two types of magnetic elastomers were analyzed: polymerized in zero field and polymerized in magnetic field. For each type there were three different mass concentrations investigated: 25%, 50% and 75% respectively. The magnetic field applied is:  $B = 156.5$  mT for each concentration. The polymer matrix consist of: a) Paste: Alpha Omega polydimethylsiloxane –  $[\text{Si}(\text{CH}_3)_2\text{O}]_n$ , calcium carbonate –  $\text{CaCO}_3$ , pigments, taste ingredients and b) Catalyst: dibutyltindilaureate, benzyl silicate, pigments.

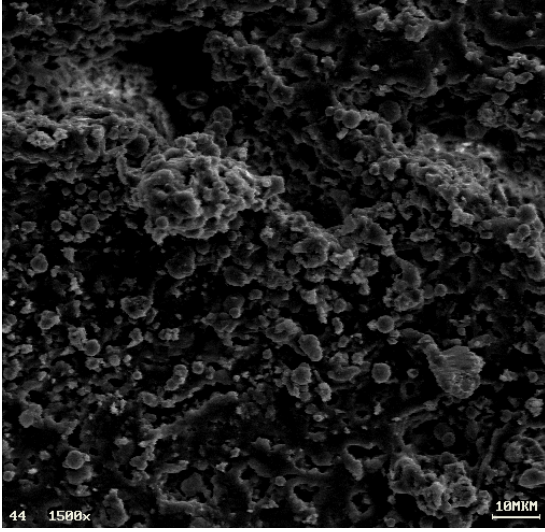


Fig. 1. Stomaflex crème + 25% Fe particles.

Scanning electron microscopy images were obtained on Fe particles for determining the size distribution of the magnetic particles. They were analyzed using a MCID Image Analyzer Software [7]. By processing these images, a distribution [Fig. 3], of the particles with the parameters: mean radius  $R = 2.09 \mu\text{m}$ , standard deviation  $\sigma = 0.26 \mu\text{m}$ , minimum radius  $R_{\text{min}} = 1.58 \mu\text{m}$  and maximum radius  $R_{\text{max}} = 2.85 \mu\text{m}$  was determined.

Small-angle neutron scattering experiments of nonpolarized neutrons were carried out at YUMO small-angle time-of-flight diffractometer [8, 9] at the IBR-2 pulsed reactor, JINR, Dubna, Russia. A two-detector system was used. The differential cross-section per sample volume (scattering intensity) isotropic over the radial angle on the detector was obtained as a function of the module of momentum transfer,  $q = (4\pi/\lambda) \sin(\theta/2)$ , where  $\lambda$  is the incident neutron wavelength and  $\theta$  is the scattering angle.

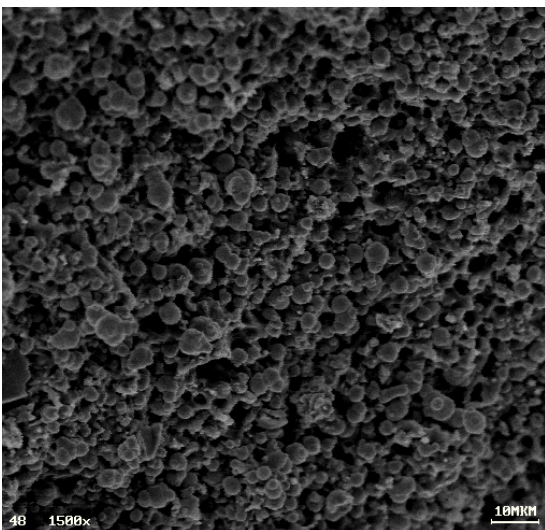


Fig. 2. Stomaflex crème + 75% Fe particles.

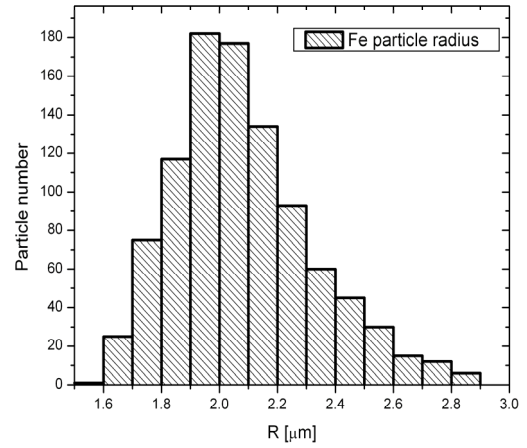


Fig. 3. Size distributions of Fe particles from EM images.

The neutron wavelengths within an interval of 0.05 – 0.5 nm were used to obtain scattering curves [Fig. 4-8,] in a  $q$ -range of 0.006 – 0.12  $\text{\AA}^{-1}$ . The wavelength of the scattered neutrons registered by the detector was determined according to the time-of-flight method. The calibration procedure was made using vanadium.

Processing of the measured spectrum, calculation of the spectrometer resolution function, data correction, carrying out the normalization of the spectrum and subtraction of the background sample data were realized using SAS [10] software program.

### 3. Theory

The scattered intensity on an absolute scale for any interacting particulate systems of scatterers can be expressed as [11]:

$$I(q) = (\Delta\rho)^2 V_p^2 N_p \langle P(q) \rangle S(q) \quad (1)$$

where:  $\Delta\rho = \rho_{\text{Fe}} - \rho$  is the scattering contrast; and  $\rho_{\text{Fe}}$  and  $\rho$  are the scattering length densities of the Fe particles and polymer matrix respectively.  $\langle \dots \rangle$  denotes a statistical average and is taken over the available positions and orientations of the particles.  $V_p$  is the mean particle volume,  $N_p$  is the number of particles per unit volume,  $P(q)$  is the scattering form factor for particles given by [2]:

$$P(q) = \left| \frac{1}{V_p} \int_{V_p} e^{i\vec{q}\cdot\vec{r}} d\vec{r} \right|^2 \quad (2)$$

and  $S(q)$  is the structure factor (the inter-particle correlation factor) [2]:

$$S(q) = 1 + 4\pi \frac{N_p}{V} \int_0^\infty [g(r) - 1] r^2 \frac{\sin(qr)}{qr} dR \quad (3)$$

and is the Fourier transform of the pair distribution function  $g(r)$  related to the probability of finding the centre of any particle at a distance  $R$  from the center of a given particle. For  $N$  particles in a volume  $V$ ,  $(N/V)g(R)dV$  is the number of particles in volume element  $dV$  at a distance  $R$  from a given particle [2].

For spherical particles, the form factor from eq. 2 has the expression [12]:

$$P(q) = \frac{3}{(qR)^3} (\sin(qR) - qR \cos(qR))^2 \quad (4)$$

The range we are concerned with for determination of specific surface is the so-called Porod regime, where the small-angle scattered component follows a  $q^{-4}$  power law whose intensity is proportional to the surface area of the interface between the scattering microstructural phases of interest. In the Porod regime, scattering from the porous material follows the Porod equation [13]:

$$I(q) = \frac{2\pi(\Delta\rho)^2 S}{q^4 V} + B \quad (5)$$

where  $\frac{S}{V}$  is the total area of the interface region per unit of volume of the particle and  $B$  is the background. Knowing the shape of the particles we are able to determine their dimensions.

#### 4. Results and discussion

Scattering length density is defined as the ratio of the scattering length per molecule and molecular volume. Having an  $X_m Y_n$  molecule, the scattering length density is given by:

$$\rho_{X_m Y_n} = \frac{mb_X + nb_Y}{v} \quad (7)$$

here  $mb_X + nb_Y$  is the scattering length per molecule and  $v$  is the volume of molecule  $X_m Y_n$  comprising  $m$  atoms  $X$  and  $n$  atoms  $Y$ . The molecular volume  $v$  is given in terms of density  $d$  and molar mass  $m$  for molecule  $X_m Y_n$  and Avogadro's number:

$$v = \frac{m}{N_{av} d} \quad (8)$$

For Fe particles the density is  $d = 7.874 \text{ g/cm}^3$ , the molar mass is:  $m = 55.85 \text{ g/mol}$ , the scattering length is:  $b_{Fe} = 9.45 \times 10^{-13} \text{ cm}$  [14], so the molecular volume is:  $v = 1.18 \times 10^{-23} \text{ cm}^3$  and  $\rho_{Fe} = 8.01 \times 10^{10} \text{ cm}^{-2}$ . Proceeding in a similar way, for the polymer matrix:  $\rho = 0.06 \times 10^{10} \text{ cm}^{-2}$  so the scattering contrast is:  $\Delta\rho = 7.95 \times 10^{10} \text{ cm}^{-2}$ .

Fig. 4, within the limits of coherent/incoherent scattering, shows the SANS data for Stomaflex crème (lower curve) and Fe particles (upper curve). The

scattering intensity for Stomaflex crème reveal a power-law behavior of the form  $I(q) \sim q^{-\alpha}$  with the exponent  $\alpha$  less than 4. From this value we obtain the fractality dimension of the polymer network. In our case ( $\alpha < 4$ ) the fractal dimension is given by:  $D_S = 6 - \alpha$  and the polymer matrix exhibits the behavior of a surface fractal object with the fractal dimension  $D_S = 2.47 \pm 0.01$ , an intermediate value between perfectly smooth surfaces ( $D_S = 2$ ) and surfaces so folded that they almost completely fills the space ( $D_S = 3$ ).

The SANS curve for Fe particles show also a power-law behavior, but here, on the linear portion of the curve, the slope has a value of 4 showing a sharp interface between the phases. For the low  $q$ -values it is seen [Fig. 4] that scattered intensity does not satisfy Porod law  $\sim q^{-4}$  and has higher values due to appearance of the structure factor. This is explained by the formation of aggregates between Fe particles and deviations from the Porod law is a measure of the interaction of particles inside the aggregates which, as a consequence shows the presence of this structure factor. Deviation from the Porod law gives strong evidence for aggregation formation. We made a fit, in log-log coordinates, for Fe particles [Fig. 4] using the model from eq. 5. The obtained value for the the surface area is:  $\frac{S}{V} = 0.75 \cdot 10^4 \text{ cm}^{-1}$  and a mean value of radius of particle  $R = 2.00 \pm 0.25 \mu\text{m}$  which are in very good agreement with electron microscopy data.

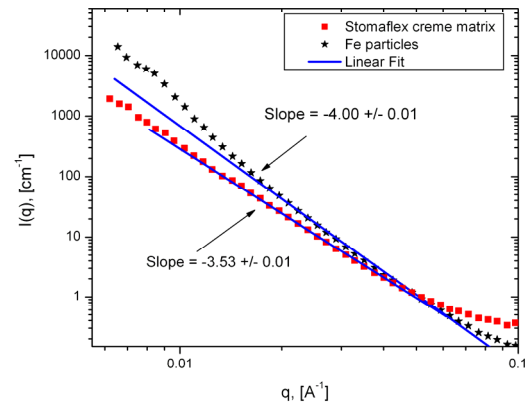


Fig. 4. Experimental curves for Fe particles, polymer matrix and linear fits.

Figs. 5 and 6 shows SANS data from magnetic elastomers polymerized without and with magnetic field. From Fig. 5 and 6 we can observe that the SANS scattered intensities increase proportionally with increasing the mass-concentration of Fe particles inside the magnetic elastomer. Scattering curves for 25%, 50% and 75% Fe concentrations can be expressed as an addition [Fig.5 and 6] of scattering curves from Fe particles and from polymer matrix [Fig. 4]. The profiles of the curves [Fig. 5] have a similar behavior for each concentration showing that in a  $q$ -range from  $0.006 \text{ A}^{-1}$  up to  $0.1 \text{ A}^{-1}$ , the microstructure of magnetic elastomers is the same. A similar effect takes place in magnetic elastomers polymerized in magnetic field [Fig. 6].

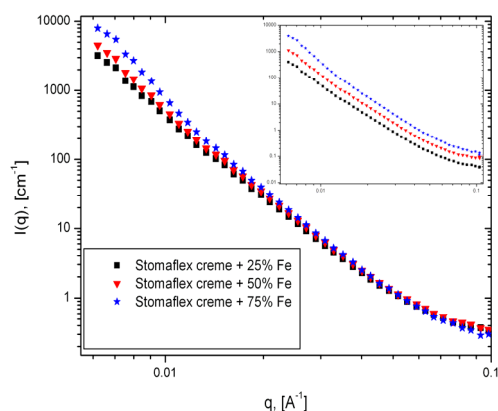


Fig. 5. Experimental curves for magnetic elastomers polymerized in zero magnetic field. Inset graphs shows the same curves scaled down by a factor of 2 for 50% Fe and by a factor of 4 for 25% Fe, as compared to curve for 75% Fe concentration.

The influence of the Fe particles on the scattering from magnetic elastomers is obtained from subtraction of the polymer matrix scattering curve [Fig. 1] from magnetic elastomer scattering curves [Fig. 5 and Fig. 6], for every concentration.

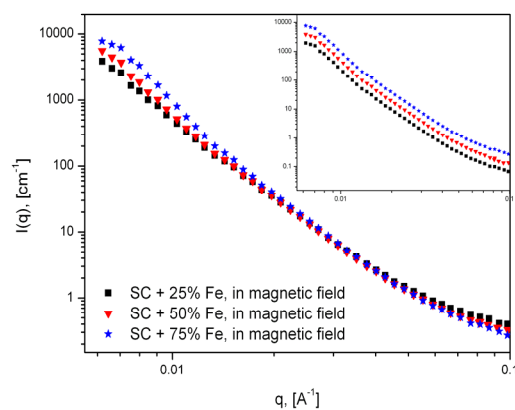


Fig. 6. Experimental curves for magnetic elastomers polymerized in magnetic field,  $B = 156.5$  mT. Inset graphs shows the same curves scaled down by a factor of 2 for 50% Fe and by a factor of 4 for 25% Fe, as compared to curve for 75% Fe concentration.

The subtraction was carried out taking into account the percent of Fe particles inside the magnetic elastomers. Figs. 7 and 8 present the results of this subtraction.

As for pure Fe particles, the scattering from Fe particles inside the elastomer deviate from the Porod law, for low  $q$  values, revealing a homogeneous distribution of aggregates inside the polymer matrix.

The profiles of the curves are the same for each concentration showing that for these sizes of particles, in a  $q$ -range of  $0.006 - 0.1$   $\text{\AA}^{-1}$  and polymerization process in a magnetic field of  $B = 156.5$  mT the microstructure of magnetic elastomers is the same, the curves being

determined by the contribution of the components parts through addition.

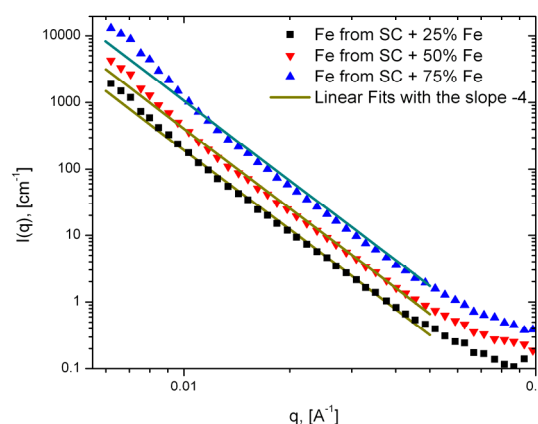


Fig. 7. Scattering curves for magnetic elastomers with various Fe concentrations ( $B = 0$ , only Fe particles contribution).

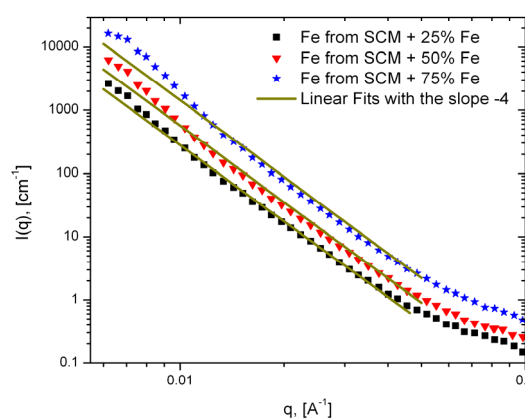


Fig. 8. Scattering curves for magnetic elastomers with various Fe concentrations ( $B = 156.6$  mT, only Fe particles contribution).

## 5. Conclusions

Electron Microscopy images of magnetic elastomers reveal the existence of Fe particles with a mean radius of  $R = 2.09$   $\mu\text{m}$  and standard deviation  $\sigma = 0.26$   $\mu\text{m}$ .

With Porod law we have determined a mean radius for particles of  $R = 2.00 \pm 0.25$   $\mu\text{m}$ , in very good agreement with scanning electron microscopy data. The scattered intensity increases proportionally with increasing the mass-concentration of Fe particles inside the magnetic elastomer for both types, polymerized with and without magnetic field. Polymer matrix exhibits the behavior of a fractal object with the surface fractal dimension  $D_s = 2.47 \pm 0.01$ .

The similarities of the scattering curves of Fe particles from magnetic elastomers polymerized without [Fig. 5] and with magnetic field of  $B = 156.5$  mT [Fig. 6] respectively, are probably due to the partial compensation of low (residual) magnetic moments. The effects

associated to a magnetic ordering are possible for  $q$ -values much smaller than  $0.006 \text{ \AA}^{-1}$  (which corresponds to dimensions greater than  $1000 \text{ \AA}$ ).

Deviations from Porod law of the scattered intensity from Fe particles are explained by the interaction of particles inside the aggregates. The same deviations appear in scattering from Fe particles after subtracting them from Stomaflex crème polymerized with and without magnetic field, respectively.

Dependence of the specific surface behavior from the size of particles in such systems is planned for future investigations.

### Acknowledgments

E.M. Anitas gratefully acknowledge the help of Dr. A. Kh. Islamov and Dr. M. L. Crauss for many usefully discussions, the support from the grant No. 3805-3-07/08 of the Romanian Governmental Representative at JINR and the support from the theme 01-3-1030-99/2008.

### References

- [1] J. Brandrup, E. H. Immergut, E. A. Grulke – “Polymer Handbook”, Wiley-Interscience; 4<sup>th</sup> edition, 1999.
- [2] P. Lindner, Th. Zemb – “Neutron, X-Rays and Light Scattering: Scattering Methods Applied to Soft Condensed Matter”, North-Holland, 2002.
- [3] J. S. Higgins, H. C. Benoit – “Polymers and Neutron Scattering in Condensed Matter”, Clarendon Press, 1994.
- [4] R. J. Roe – “Methods of X-Rays and Neutron Scattering in Polymer Science”, Oxford University Press, 2000.
- [5] L. A. Feigin, D. I. Svergun – “Structure Analysis by Small-Angle X-Ray and Neutron Scattering”, New-York: Plenum Press, 1987.
- [6] I. Bica – Mater. Sci. Eng. **B98**, 89 (2003).
- [7] <http://www.mcid.co.uk>
- [8] Yu. M. Ostanevich – Makromol. Chem. Macromol. Symp. **15**, 91 (1998).
- [9] A. I. Kuklin, A. Kh. Islamov, V. I. Gordeliy – Neutron News, **16**(3), 16 (2005).
- [10] A. G. Soloviev, T. M. Solovieva, A. V. Stadnik, A. Kh. Islamov, A. I. Kuklin – JINR preprint **P10-2003-86**.
- [11] J. P. Hansen, J. A. McDonald – “Theory of Simple Liquids”, 3<sup>rd</sup> Ed., Academic Press, 2006.
- [12] A. Guinier, G. Fournet, - “Small-Angle Scattering of X-Rays”, New York: John Wiley and Sons, 1955.
- [13] G. Porod, Kolloid Z. **124**, 83 (1951).
- [14] V. F. Sears - Neutron News, **3**(3), 29 (1992).

\*Corresponding author: [anitas@theor.jinr.ru](mailto:anitas@theor.jinr.ru)